Communication

Correlating the Crystal Structure of A Thiol-Protected Au Cluster and Optical Properties

Manzhou Zhu, Christine M. Aikens, Frederick J. Hollander, George C. Schatz, and Rongchao Jin

J. Am. Chem. Soc., **2008**, 130 (18), 5883-5885 • DOI: 10.1021/ja801173r • Publication Date (Web): 12 April 2008

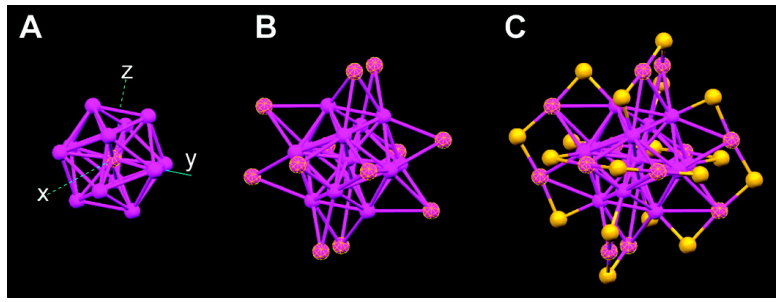

More About This Article

Additional resources and features associated with this article are available within the HTML version:

- Supporting Information
- Links to the 18 articles that cite this article, as of the time of this article download
- Access to high resolution figures
- Links to articles and content related to this article
- Copyright permission to reproduce figures and/or text from this article

View the Full Text HTML

J|A|C|S
COMMUNICATIONS

Published on Web 04/12/2008

Correlating the Crystal Structure of A Thiol-Protected Au_{25} Cluster and Optical Properties

Manzhou Zhu,[†] Christine M. Aikens,[‡] Frederick J. Hollander,[§] George C. Schatz,[||] and Rongchao Jin*,[†]

Department of Chemistry, Carnegie Mellon University, 4400 Fifth Avenue, Pittsburgh, Pennsylvania 15213, Department of Chemistry, Kansas State University, Manhattan, Kansas 66506, College of Chemistry, University of California at Berkeley, Berkeley, California 94720, Department of Chemistry, Northwestern University, Evanston, Illinois 60208

Received February 15, 2008; E-mail: rongchao@andrew.cmu.edu

Thiol-stabilized gold nanoparticles, including nanocrystals and nanoclusters, have attracted significant research interest in nanoscience in recent years due to their importance in both fundamental science[1–11] and technological applications such as catalysis,[12] optics,[13] biomedicine,[14] and chemical sensing.[15] When the size of gold nanoparticles approaches the de Broglie wavelength of the conduction electrons (~1 nm diameter), the quasicontinuous electronic bands in bulk gold or large nanoparticles (>5 nm) evolve to discrete levels. Small gold nanoparticles (<3 nm) lose their bulk-like electronic properties; for example, they no longer support the plasmon excitation characteristic of relatively large gold nanocrystals (3−100 nm).[16,17] In addition, the atomic packing mode in small metal nanoparticles (also called clusters) plays an important role in their structure−property correlations and their size dependent properties.[18–22] The transition from the cluster state to the nanocrystalline state raises a number of fundamental questions, such as how the discrete electronic states develop into the collective plasmon state as the cluster size increases and what kind of atomic packing modes may exist in clusters. For the latter, a ubiquitous structural motif—the centered icosahedron, and a golden rule of "cluster of clusters" have previously been discovered in a series of Au/Ag-containing alloy clusters stabilized by phosphines.[23]

With respect to thiol-protected gold clusters, despite the great advances that have been achieved in the past decade in the synthesis of such clusters,[1–11,24–27] significant challenges still remain, such as the unambiguous determination of the cluster size (i.e., the number of gold atoms) and atomic packing in the cluster. To determine their exact size and structure via X-ray crystallography, the ultimate approach is to grow single crystals of gold-thiolate clusters; this unfortunately has long been a big challenge. Thus far, there has been only one example of an Au-thiolate cluster, Au_{102}(*p*-mercaptobenzoic acid)$_{44}$, that has been crystallographically determined.[28] The Au_{102} clusters have a 49-atom Marks decahedral core, which could also be considered to be a five-twinned face-centered cubic or hexagonal close-packed core. To explore the potential unique structure and physical and chemical properties of gold clusters, clusters comprising a few dozen atoms should be further pursued.

Herein we report the unusual single crystal structure of a phenylethanethiol-capped, 25-atom gold cluster.[36] We have correlated this structure with its optical absorption spectrum by performing time-dependent density functional theory (TDDFT) calculations. The structure of the Au_{25} thiolate cluster has been long sought since the initial synthesis of this cluster nearly a decade ago.[24–27] In our work, attainment of the crystal structure was facilitated by an improved kinetically controlled synthesis method that leads to monodisperse cluster formation[29] (see Supporting Information for crystallization details).

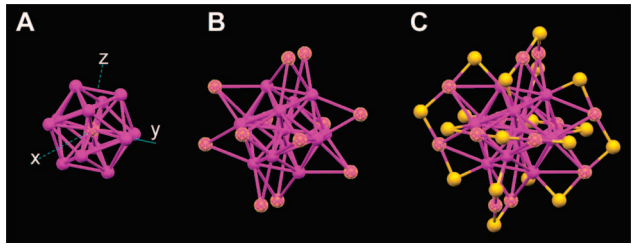

Figure 1. Crystal structure of a $Au_{25}(SR)_{18}$ cluster (R is phenylethyl group): (A) the icosahedral Au_{13} core; (B) the Au_{13} core plus the exterior 12 Au atoms; (C) the whole Au_{25} cluster protected by 18 thiolate ligands (for clarity, only S was shown, magenta, Au; yellow, S).

X-ray crystallographic analysis shows that the Au_{25} cluster is based on a centered icosahedral Au_{13} core (Figure 1A), which is capped by an exterior shell composed of the remaining twelve Au atoms, and the whole cluster is encapsulated by eighteen thiolate ligands. The best way to appreciate the symmetry of the Au_{25} cluster is to view them along the 2-fold axes of the icosahedron (*x*, *y*, and *z*, Figure 1A). If one takes three mutually perpendicular 2-fold axes of the icosahedron (the D_2 subset of the O_h symmetry), one can readily define how the remaining twelve Au atoms are situated, that is, they are in six pairs around each 2-fold axis (Figure 1B); overall, the twelve exterior Au atoms form an incomplete shell, leaving eight Au_3 faces of the icosahedron uncapped (note that an icosahedron possesses 20 triangular faces). For each exterior Au atom, there is one shorter Au−Au contact (3.02−3.12 Å) to the Au_{13} icosahedron and two longer ones (3.14−3.27 Å) to the other two Au atoms on the face it is capping. Bond distances on the surface of the icosahedron obey approximate D_{2h} symmetry with the three unique bonds being significantly shorter (2.80−2.81 Å) than the others (average 2.95 Å).

The bonding between the thiolate ligands and gold atoms is also particularly interesting, Figure 1C. For clarity, the phenylethyl groups are omitted. All the thiolate ligands adopt a bridging bonding mode rather than a terminal one as is the case with monodentate phosphine ligands.[18–23] Each of the exterior Au−Au pairs (six in total) is bridged by an −SR ligand and with two other −SR ligands bridging between the exterior Au

[†] Carnegie Mellon University.
[‡] Kansas State University.
[§] University of California at Berkeley.
[||] Northwestern University.

10.1021/ja801173r CCC: $40.75

atoms and the icosahedral core. Thus, the Au_{25} cluster is capped by eighteen −SR ligands. The bridging mode of the thiolate ligands is related to that observed recently for Au_{102}(*p*-mercaptobenzoic acid)$_{44}$ clusters.[28] However, in the $Au_{25}(SR)_{18}$ cluster the bridging −SR ligands form an extended "staple" motif, where three sulfur and two gold atoms are arranged in a 'V-shaped' −S−Au−S−Au−S− pattern (Figure 1C and Supporting Information, Figure S1). This extended motif binds to the icosahedral core through S−Au and Au−Au bonds, which is in contrast with $Au_{102}(SR)_{44}$, in which a simple "staple" motif (−S−Au−S−) was found to bind to interior Au atoms.[28] There are also additional features worthy of mention in the $Au_{25}(SR)_{18}$ structure. If one views the atomic plane along the 2-fold axes, for example, the $y-z$ plane (Figure S1), the S atoms (no. 1 and 1′) are slightly bent out of the plane (Figure S1-B). For the −S−Au−S−Au−S− motif (Figure S1-A), the α-C bonded to sulfur no. 1 points down while the other two α-C bonded to sulfur no. 3 and no. 5 point up (Figure S1-B); overall, the six ligands still have an inversion symmetry.

The atomic packing mode observed in the Au_{25}-thiolate cluster was a surprise. This highly symmetric structure was not predicted by previous density functional theory (DFT) calculations, which considered the possibilities of a face-centered-cubic core or a biicosahedral Au_{25} core,[30] and it also violates the empirical golden rule, cluster of clusters, which would predict a biicosahedral structure.[23] With respect to the structures of phosphine-protected metal clusters, in early work Teo and coworkers reported the observation of a common structural motif, icosahedron (composed of 13 metal atoms) in various phosphine-capped gold/silver bimetallic clusters.[31] They proposed a rule: cluster of clusters via vertex sharing of icosahedral M_{13} building blocks.[23,31] This empirical rule successfully accounted for a variety of observed structures of high nuclearity phosphine-capped clusters, for example, biicosahedral $[(p\text{-}tol_3P)_{10}Au_{13}Ag_{12}Br_8]^+$, triicosahedral $[(p\text{-}tol_3P)_{12}Au_{18}Ag_{20}Cl_{14}]^+$, tetraicosahedral $[(Ph_3P)_{12}Au_{22}Ag_{24}Cl_{10}]$ clusters.[23,31] In particular, for 25-atom clusters, the biicosahedral structure was demonstrated to be a ubiquitous one, which was observed in several series of bimetallic (e.g., $Au_{13}Ag_{12}$, $Au_{12}Ag_{13}$) and trimetallic (e.g., $Au_{12}Ag_{12}Pt$, $Au_{11}Ag_{12}Pt_2$, $Au_{12}Ag_{12}Ni$) clusters.[31] Interestingly, such a biicosahedral structure was also observed in a mixed ligand (triphenylphosphine and alkanethiol)-capped Au_{25} cluster;[32] in this case the five thiolate ligands were found to be on the bridges connecting two pentagons from the two icosahedra. In our work, the unexpected structure observed in all-thiolate protected Au_{25} clusters indicates that the core structure of gold clusters may be significantly affected by the bonding mode between ligands and gold atoms. The highly symmetric structure of Au_{25}-thiolate clusters accounts for their excellent chemical stability, albeit the outer shell (twelve Au atoms) does not form a closed shell; eight more Au atoms would be needed to cap all the faces of the icosahedral core.

Both X-ray crystallographic and NMR analyses of the Au_{25} cluster reveal that one equivalent of tetraoctylammonium cations (a phase transfer agent used in the synthesis) accompanies the $Au_{25}(SR)_{18}$ clusters, indicating that the cluster is an anion, $Au_{25}(SCH_2CH_2Ph)_{18}^-$. Because of strong quantum size effects, the Au_{25} cluster shows multiple molecular-like transitions in their optical absorption spectrum; at least three well-defined bands at 1.8, 2.75, and 3.1 eV were observed in the UV−vis spectrum (Figure 2). This optical behavior is fundamentally different from gold nanocrystals (>3nm), the latter typically show a collective electron excitation mode−surface plasmon resonance at ∼2.4 eV for spherical particles (3−30 nm).[17] It is

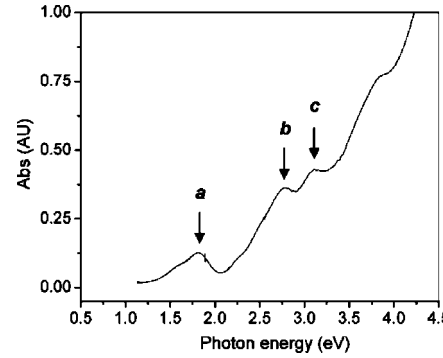

Figure 2. The UV−vis spectrum of Au_{25} clusters (single crystals redissolved in toluene). No Jacobian correction was done.

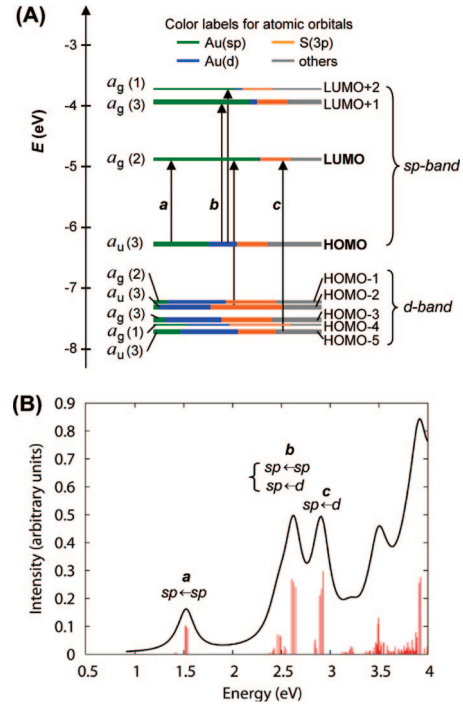

Figure 3. (A) Kohn−Sham orbital energy level diagram for a model compound $Au_{25}(SH)_{18}^-$. The energies are in units of eV. Each KS orbital is drawn to indicate the relative contributions (line length with color labels) of the atomic orbitals of Au (6sp) in green, Au (5d) in blue, S (3p) in yellow, and others in gray (those unspecified atomic orbitals, each with a < 1% contribution). The left column of the KS orbitals shows the orbital symmetry (g, u) and degeneracy (in parenthesis); the right column shows the HOMO and LUMO sets. (B) The theoretical absorption spectrum of $Au_{25}(SH)_{18}^-$. Peak assignments: peak a corresponds to 1.8 eV observed, peak b corresponds to 2.75 eV (observed), and peak c corresponds to 3.1 eV (observed).

evident that quantum size effects dominate the absorption behavior of gold clusters composed of a few dozen atoms.

To correlate the cluster structure and optical properties, we have performed time-dependent density functional theory (TD-DFT) calculations (see Supporting Information and ref 33) for the electronic structure and optical absorption spectrum of $Au_{25}(SH)_{18}^-$ as a model. The Kohn−Sham molecular orbitals (MO), energies, and atomic orbital (AO) contributions are shown in Figure 3A (see Table S1 for numerical values). In the electronic structure of $Au_{25}(SH)_{18}^-$, the HOMO and the lowest three LUMOs are mainly composed of 6sp atomic orbitals (labeled in green) of gold, thus, these orbitals constitute the sp-band (Figure 3A). The HOMO-1 through HOMO-5 are mainly

constructed from the $5d^{10}$ atomic orbitals (labeled in blue) of gold and hence constitute the d-band. Note that both sets of HOMO and LUMO orbitals have a significant degree of the S(3p) (labeled in yellow) character. In addition, the HOMO level is triply degenerate while the LUMO is doubly degenerate.

The theoretical spectrum for $Au_{25}(SH)_{18}^-$ agrees quite well with experiment, especially in the spectral shape (compare Figure 3B and Figure 2). The first excited state occurs at 1.52 eV (peak *a* in Figure 3B) and corresponds to a LUMO ← HOMO transition (Figure 3A), which is essentially an intraband (*sp* ← sp) transition. Because in the HOMO series only the three KS orbitals in the HOMO (triply degenerate) have more s character than d character, transitions arising out of the other occupied HOMO-*n* orbitals tend to be interband (sp ← d) transitions (Figure 3A). The peak at 2.63 eV (*b* in Figure 3B) arises from mixed intraband (sp ← sp) and interband (sp ← d) transitions (Figure 3A). The peak at 2.91 eV (*c* in Figure 3B) arises principally from an interband transition (sp ← d). Of note, the HOMO, LUMO, and other orbitals including the HOMO−1 and LUMO+1 are composed almost exclusively of AO contributions from the 13 Au atoms in the icosahedral core rather than the 12 exterior Au atoms. Thus, the first peak in the absorption spectrum (*a* in Figure 2 and Figure 3) can be viewed as a transition that is due entirely to the electronic and geometric structure of the Au_{13} core. This is strikingly different from a biicosahedral structure; the latter shows a similar low energy band at 1.76 eV, but its origin is attributed to the interaction between the two vertex-sharing Au_{13} icosahedra rather than the electronic transition within the individual Au_{13} unit.[30,34] These results clearly demonstrate that the cluster structure plays an important role in optical properties.

The model compound $Au_{25}(SH)_{18}^-$ exhibits peaks in the optical absorption spectrum that lie uniformly to the red of the corresponding peaks in experiment. The set of occupied orbitals (HOMO through HOMO−5) have a significant degree of sulfur character (∼25−40%), while the unoccupied orbitals (LUMO through LUMO+2) have a smaller percentage (∼15−20%) (Figure 3A). The increased electron donation from the CH_2CH_2Ph moieties in $Au_{25}(SCH_2CH_2Ph)_{18}^-$ would lead to orbital energies that are more negative for orbitals with significant ligand character, which would thus increase the HOMO−LUMO gap and lead to a blue-shift in the absorption spectrum, hence, closer to experiment. Such an effect was observed in $Au_{20}(PH_3)_4$, the LUMOs have a significant degree of phosphorus character;[35] the HOMO−LUMO gap for $Au_{20}(PH_3)_4$ is predicted to be 1.44 eV, while the gap for $Au_{20}(PPh_3)_4$ is predicted to be 1.82 eV due to the increased electron donation by triphenylphosphine ligands.[35] Of course errors in TDDFT may also play a role in the differences between theory and experiment.

The crystal structure observed in the $Au_{25}(SR)_{18}$ cluster could indicate a plausible cluster growth pattern in which an Au_{13} icosahedron was first formed, followed by subsequent atom-by-atom growth pathway. Herein, an intriguing question arises, that is, why the "cluster of clusters" growth pathway (i.e., two Au_{13} icosahedra forming a biicosahedron via vertex-sharing) is inhibited. We believed this is caused by the bridging mode of bonding of the thiol ligands. To answer this and many other fundamental questions, it is of paramount importance to prepare a series of size discrete gold-thiolate clusters and to crystallographically characterize their structures, in particular in the range of ∼10 to ∼100 atoms, since the transitions in terms of structures and material properties are expected to occur within this range. Correlation between experimental and theoretical geometric and electronic structure information may lead to a fundamental understanding of the factors that lead to exceptionally stable gold thiolate clusters, as well as the origin of collective plasmon excitations in metal nanocrystals.

Acknowledgment. R.J. acknowledges the CMU startup and AFOSR (9550-07-1-0245) for supporting this research; C.M.A. acknowledges support from Kansas State University; G.C.S acknowledges NSF Grant CHE-0550497. We thank Prof. Nathaniel Rosi for kindly collecting the single crystal preliminary X-ray diffraction data and helpful discussions.

Supporting Information Available: Experimental details, X-ray crystallographic analysis, and DFT calculation; Figure S1, S2, Table S1 and S2, and CIF file of the cluster. This material is available free of charge via the Internet at http://pubs.acs.org.

References

(1) Alvarez, M. M.; Khoury, J. T.; Schaaff, T. G.; Shafigullin, M.; Vezmar, I.; Whetten, R. L. *Chem. Phys. Lett.* **1997**, *266*, 91.
(2) Brust, M.; Fink, J.; Bethell, D.; Schiffrin, D. J.; Kiely, C. *J. Chem. Soc., Chem. Commun.* **1995**, 1655.
(3) (a) Ingram, R. S.; Hostetler, M. J.; Murray, R. W. *J. Am. Chem. Soc.* **1997**, *119*, 9175. (b) Chen, S. W.; Ingram, R. S.; Hostetler, M. J.; Pietron, J. J.; Murray, R. W.; Schaaff, T. G.; Khoury, J. T.; Alvarez, M. M.; Whetten, R. L. *Science* **1998**, *280*, 2098.
(4) Cleveland, C. L.; Landman, U.; Schaaff, T. G.; Shafigullin, M. N.; Stephens, P. W.; Whetten, R. L. *Phys. Rev. Lett.* **1997**, *79*, 1873.
(5) Schmidbaur, H., Ed. *Gold: Progress in Chemistry, Biochemistry, and Technology*; Wiley: New York, 1999.
(6) Wang, G.; Huang, T.; Murray, R. W.; Menard, L.; Nuzzo, R. G. *J. Am. Chem. Soc.* **2005**, *127*, 812.
(7) Yang, Y.; Chen, S. *Nano Lett.* **2003**, *3*, 75.
(8) Wilcoxon, J. P.; Provencio, P. *J. Phys. Chem. B* **2003**, *107*, 12949.
(9) Negishi, Y.; Nobusada, K.; Tsukuda, T. *J. Am. Chem. Soc.* **2005**, *127*, 5261.
(10) Nunokawa, K.; Onaka, S.; Ito, M.; Horibe, M.; Yonezawa, T.; Nishihara, H.; Ozeki, T.; Chiba, H.; Watase, S.; Nakamoto, M. *J. Organomet. Chem.* **2006**, *691*, 638.
(11) Jin, R.; Egusa, S.; Scherer, N. F. *J. Am. Chem. Soc.* **2004**, *126*, 9900.
(12) Zheng, N.; Stucky, G. D. *J. Am. Chem. Soc.* **2006**, *128*, 14278.
(13) Fan, H.; Yang, K.; Boye, D. M.; Sigmon, T.; Malloy, K. J.; Xu, H.; López, G. P.; Brinker, C. J. *Science* **2004**, *304*, 567.
(14) Rosi, N. L.; Giljohann, D. A.; Thaxton, C. S.; Lytton-Jean, A. K. R.; Han, M. S.; Mirkin, C. A. *Science* **2006**, *312*, 1027.
(15) Wohltjen, H.; Snow, A. W. *Anal. Chem.* **1998**, *70*, 2856.
(16) Wyrwas, R. B.; Alvarez, M. M.; Khoury, J. T.; Price, R. C.; Schaaff, T. G.; Whetten, R. L. *Eur. Phys. J. D* **2007**, *43*, 91.
(17) Kelly, K. L.; Coronado, E.; Zhao, L. L.; Schatz, G. C. *J. Phys. Chem. B* **2003**, *107*, 668.
(18) de Silva, N.; Dahl, L. F. *Inorg. Chem.* **2005**, *44*, 9604.
(19) Teo, B. K.; Shi, X.; Zhang, H. *J. Am. Chem. Soc.* **1992**, *114*, 2743.
(20) Bertino, M. F.; Sun, Z.-M.; Zhang, R.; Wang, L.-S. *J. Phys. Chem. B* **2006**, *110*, 21416.
(21) Schmid, G., Ed. *Clusters and Colloids;* VCH: Weinheim, Germany, 1994.
(22) Mingos, D. M. P. *Polyhedron* **1984**, *3*, 1289.
(23) Teo, B. K.; Zhang, H. *Coord. Chem. Rev.* **1995**, *143*, 611.
(24) Schaaff, T. G.; Knight, G.; Shafigullin, M. N.; Borkman, R. F.; Whetten, R. L. *J. Phys. Chem. B* **1998**, *102*, 10643.
(25) Donkers, R. L.; Lee, D.; Murray, R. W. *Langmuir* **2004**, *20*, 1945.
(26) Wang, W.; Murray, R. W. *Langmuir* **2005**, *21*, 7015.
(27) Negishi, Y.; Chaki, N. K.; Shichibu, Y.; Whetten, R. L.; Tsukuda, T. *J. Am. Chem. Soc.* **2007**, *129*, 11322.
(28) Jadzinsky, P. D.; Calero, G.; Ackerson, C. J.; Bushnell, D. A.; Kornberg, R. D. *Science* **2007**, *318*, 430.
(29) Zhu, M.; Lanni, E.; Garg, N.; Bier, M. E.; Jin, R. *J. Am. Chem. Soc.* **2008**, *130*, 1138.
(30) Iwasa, T.; Nobusada, K. *J. Phys. Chem. C* **2007**, *111*, 45.
(31) (a) Zhang, H.; Teo, B. K. *Inorg. Chim. Acta* **1997**, *265*, 213. (b) Teo, B. K.; Shi, X. B.; Zhang, H. *J. Chem. Soc., Chem. Commun.* **1992**, 1195. (c) Teo, B. K.; Zhang, H.; Shi, X. *Inorg. Chem.* **1994**, *33*, 4086.
(32) Shichibu, Y.; Negishi, Y.; Watanabe, T.; Chaki, N. K.; Kawaguchi, H.; Tsukuda, T. *J. Phys. Chem. C* **2007**, *111*, 7845.
(33) Aikens, C. M.; Schatz, G. C. *J. Phys. Chem. A* **2006**, *110*, 13317.
(34) Nobusada, K.; Iwasa, T. *J. Phys. Chem. C* **2007**, *111*, 14279.
(35) (a) Aikens, C. M.; Schatz, G. C. Time-Dependent Density Functional Theory Examination of the Effects of Ligand Adsorption on Metal Nanoparticles,*ACS Symp Ser.*, Chapter 9, in press. (b) Zhang, H.-F.; Stender, M.; Zhang, R.; Wang, C.; Li, J.; Wang, L.-S. *J. Phys. Chem. B* **2004**, *108*, 12259.
(36) It was brought to our attention that during the review process of this work, two closely related reports appeared: (a) Heaven, M. W.; Dass, A.; White, P. S.; Holt, K. M.; Murray, R. W. *J. Am. Chem. Soc.* **2008**, *130*, 3754. (b) Akola, J.; Walter, M.; Whetten, R. L.; Hakkinen, H.; Gronbeck, H. *J. Am. Chem. Soc.* **2008**, *130*, 3756.

JA801173R